Space Sciences Laboratory
Report No. SSL-81(7951)-1

ON THE STRUCTURES AND MAPPING OF AURORAL ELECTROSTATIC POTENTIALS

by

Y. T. Chiu and A. L. Newman

Space Sciences Laboratory
The Aerospace Corporation
El Segundo, California 90245

J. M. Cornwall

Department of Physics
University of California at Los Angeles
Los Angeles, California

February 1981

This work was supported in part by NASA Solar-Terrestrial Theory Program Contract NASW-3434 and in part by NASA Headquarters Contract NASW-3327.

Abstract

We examine the mapping of magnetospheric and ionospheric electric fields in a kinetic model of magnetospheric-ionospheric electrodynamic coupling proposed for the aurora by Chiu and Cornwall (1980). A new feature is the generalization of the kinetic current-potential relationship to the return-current region (identified as a region where the parallel potential drop from magnetosphere to ionosphere is positive); such a return current always exists unless the ionosphere is electrically charged to grossly unphysical values. We are able for the first time to give a coherent phenomenological picture of both the low-energy return current and the high-energy precipitation of an inverted-V. The mapping between magnetospheric and ionospheric electric fields is phrased in terms of a Green's function which acts as a filter, emphasizing magnetospheric latitudinal spatial scales of order (when mapped to the ionosphere) 50-150 km. This same length, when multiplied by perpendicular electric fields just above the ionosphere, sets the scale for parallel potential drops between the ionosphere and equatorial magnetosphere.

I. INTRODUCTION

As the result of particle and field observations in the aurora by rocket and satellite-borne instruments, it is by now fairly well-established that the auroral particles are accelerated by steady (relative to particle transit time) electric potential differences of ~ 1-10 kilovolts between the magnetosphere and ionosphere, aligned along the magnetic field [Evans, 1974; Croley et al., 1978; Mizera and Fennell, 1977; Shelley et al., 1976; Mozer et al., 1977]. These observations confirmed and refined earlier indications of possible particle acceleration in the aurora [Frank and Ackerson, 1971; Gurnett and Frank, 1973]. Consequently, recent theoretical efforts have been focused on the formation of the auroral electric acceleration potential by various kinetic mechanisms [e.g., Swift, 1975; Kan, 1975; Hudson and Mozer, 1978; Lemaire and Scherer, 1974; Chiu and Schulz, 1978; Stern, 1981] which are to be contrasted with auroral models based on MHD considerations [e.g., Sato, 1978; Miura and Sato, 1980; Goertz and Boswell, 1979]. Each of these two categories of auroral models tends to ignore what is most important in the other category and is correspondingly incomplete [Chiu et al., 1980, 1981]. In particular, most of the kinetic auroral models omit ionospheric and/or cross-field charge-separation effects, which amounts to decoupling neighboring magnetic field lines thus yielding no definite connection between parallel and perpendicular electric fields.

Recently Chiu and Cornwall [1980] initiated a program to remedy these defects, generalizing the kinetic models to account for ionospheric current conservation and charge conservation in the magnetosphere. These authors wrote down a simple differential equation in L relating the ionospheric potential to the L-dependence of the parallel potential drop between ionosphere and magnetosphere, which, in effect, specifies the mapping of magnetospheric and

ionospheric electric fields along magnetic field lines in the presence of parallel electric potential drops. This equation followed from the nearly linear relation between the current of precipitated auroral electrons at the ionosphere and the magnetosphere-ionosphere potential drop [Chiu and Cornwall, 1980; Fridman and Lemaire, 1980] predicted by kinetic theory when the mirror ratio is large. Lyons [1980, 1981] has also studied this differential equation in some detail, motivated in part by observations [Lyons et al., 1979] which confirm the linear current-potential relationship, in connection with the convection reversal boundary. (Chiu et al. [1980] have also noted the connection between auroral parallel potential drop and the convection reversal boundary). More recently, Kan and Lee [1980] have studied the problem of momentum transfer from ionosphere to magnetosphere with similar ideas.

In this paper we report on numerical and analytic investigation of electrostatic field mapping in the presence of parallel potential drops between the magnetosphere and ionosphere. In particular, we are able to consider the effects of boundary conditions such that the ionosphere is not grossly charged up. In effect, this is the condition that there is no net Pedersen current in or out of the auroral zone (assumed to circle the earth). Under these conditions, there is always a return current region. Moreover, the parallel potential drop in the return current region is typically $< (10\text{-}25)$ % of the central potential drop, so the return current is carried by relatively low-energy electrons, say tens to a few hundred eV.

We show that the general solution of our model admits potential structures which can generate both S-shape (perpendicular electric field enhancement without field reversal) and V-shape (with field reversal) "shock" structures [Temerin et al., 1981], depending primarily upon the boundary conditions assumed. Indeed, we show that the V-shaped potential structure does not

differ materially from the S-shaped structure except that imposed boundary conditions are such that in the V-shape the magnetospheric and ionospheric potential extrema are forced to lie on the same magnetic field line. This view of the relationship between the two classes of potential structures lends itself to the interpretation that one should reasonably see higher probability of occurrence for S-shapes than V-shapes. A systematic classification of model solutions and their implications on auroral return currents are given in Sections IV and V.

An important consequence of our Green's function formulation as ionospheric potential response to an imposed magnetospheric potential is that it can be directly used to map electrostatic potentials from the equator to the ionosphere by relating perpendicular electric fields to those associated with a kinetic-model magnetic field-aligned pontential drop and current. The mapping of electric fields in the magnetosphere [e.g., Mozer, 1970] and in the ionosphere-atmosphere [e.g., Chiu, 1974] is a very important problem for auroral electrodynamic observations and interpretations [e.g., Mozer, 1971]. The magnetospheric-ionospheric mapping problem for the latitudinal component of $E_\perp$ is illustrated in Figure 1. Before the advent of parallel potential drops, it was assumed that magnetic field lines were electric equipotentials (because of assumed infinite parallel conductivity); hence, electric field mapping between the magnetosphere and ionosphere was strictly geometrical depending on the distance between neighboring field lines. In other words, the scales of ionospheric electric fields were related to that of the magnetospheric fields strictly by the geometric convergence of the magnetic field, as required by $\nabla \times \vec{E} = 0$; i.e., the line integral of $\vec{E}$ along the magnetosphere-ionosphere circuit reduces to $\Delta\phi_I = \Delta\phi_M$ in Fig. 1. However, if a field-aligned potential drop such as $\Delta\phi_{IM}$ in Fig. 1 exists, the line integral

of $\vec{E}$ over the magnetosphere-ionosphere circuit not only involves $\Delta\phi_{IM}$ but also the perpendicular scale of the field-aligned currents $J_{\parallel}$ since the mapping depends on where the field lines L_1 and L_2 are located in relation to the upward and downward field-aligned currents. Roughly speaking, the scale of parallel potential drops in the auroral region is found by multiplying perpendicular equatorial magnetospheric electric fields by the usual geometric mapping factor ($\approx L^{3/2}$) and by the scale length (50-100 km) of inverted-V precipitation regions. In a later work we will take up the problem of large-scale mapping in quantitative detail.

II. CHARGE AND CURRENT CONSERVATION IN A KINETIC MODEL

In this section we give a brief summary of a kinetic model formulation of magnetosphere-ionosphere coupling leading to auroral acceleration [Chiu and Cornwall, 1980]. The basic premise is that auroral particle distributions are in quasi-static collisionless equilibrium (for time scales long compared to ion transit time) with the electric and magnetic fields. It has been pointed out by many authors [see review by Stern, 1981] that differential pitch-angle anisotropy between electrons and ions in a dipolar flux tube would lead to a magnetic field-aligned electric potential drop of several kilovolts even in a one-dimensional model in which the effects of the perpendicular electric field are ignored. Such one-dimensional models produce features of particle distribution functions in velocity space in agreement with S3-3 particle observations (Chiu and Schulz, 1978). In addition, such one dimensional models predict that the magnetic field-aligned current density $J_\parallel$ should be approximately proportional to the magnetic field-aligned potential difference between the ionosphere and the magnetosphere [Fridman and Lemaire, 1980; Chiu and Cornwall, 1980]. This relationship is in agreement with rocket observations [Lyons et al., 1979].

Chiu and Cornwall [1980] generalized such kinetic models to two-dimensions to include the influences of the perpendicular electric field by invoking kinetic charge conservation in the auroral region (Poisson's equation) and current conservation in a schematic sheet-like ionosphere with height-integrated Pedersen conductivity Σ_p. Thus, for ionospheric potential ϕ, the height-integrated current conservation equation states that

$$\nabla_\perp \cdot (\Sigma_p \nabla_\perp \phi) = -J_\parallel \ , \tag{1}$$

where $J_\parallel$ is defined to be negative for downgoing electrons. Now the kinetic models (or rocket observations) imply, aside from a term to be identified with diffuse auroral precipitation, that $J_\parallel$ is proportional to the magnetic field-aligned difference between ϕ and the electric potential at the magnetospheric equator ϕ_0,

$$- J_\parallel \approx Q\ (\phi - \phi_0) \tag{2}$$

where $Q > 0$ depends on particle densities and velocities. Equation (2) has been written down by several authors for a bi-Maxwellian distribution [Chiu and Cornwall, 1980; Fridman and Lemaire, 1980]. This remarkable linear relation between $J_\parallel$ and $\phi - \phi_0$ holds because of the smallness of the mirror ratio B_0/B_ℓ. In the Appendix we give the generalization of (2) to an arbitrary distribution function, which shows that the parameter ϕ is of order $Ne^2/M\bar{v}$, where $\bar{v}$ is a velocity typical of the given distribution function. Within the approximation made in the present paper, the properties of magnetospheric <u>particles</u> appear directly only in the parameter Q; auroral features are otherwise determined by magnetospheric perpendicular electric fields and by the ionospheric Pedersen conductivity (these latter quantities, of course, may be in part determined by the particle parameters).

Combining (1) and (2) one obtains an equation specifying the ionospheric electric-potential response ϕ to a given magnetospheric dynamo potential ϕ_0:

$$\nabla_\perp \cdot (\Sigma_p \nabla_\perp \phi) = Q\ (\phi - \phi_0) \tag{3}$$

Lyons (1980) has studied this equation, choosing ϕ_0 to represent "discontinuities in the magnetospheric convection electric field $\vec{E}$ with $\nabla \cdot \vec{E} < 0$." Lyons'

solutions show no return current region, and are based on a boundary condition of constant $\vec{E}$ at infinity, both at the ionosphere and at the magnetospheric equator. In this paper we classify and interpret solutions of (3) using the Green's function technique, and imposing the condition that the ionosphere does not become electrically charged to grossly unphysical values; our solutions are thus different from Lyons'.

Of course, equation (3) by itself tells us nothing about what happens between the equatorial magnetosphere and the top of the ionosphere. The physics of this region is largely governed by Poisson's equation and the relation between net charge density, electrostatic potential, and magnetic mirroring forces. In the presence of an inhomogeneous magnetic field, Poisson's equation reads [Chiu and Cornwall, 1980]:

$$\nabla_\perp \cdot (K\vec{E}_\perp) + B \frac{\partial}{\partial s} (B^{-1} E_\parallel) = 4\pi e (N_i - N_e) \qquad (4)$$

where N_e, N_i are complicated functions of B and ϕ, and $K \gg 1$ is the plasma dielectric constant, which depends on N_i, N_e, B and ϕ. We will not use (4) directly in the present work; for us the important consequence of (4) is that field lines are coupled, in the magnetosphere, over lengths scaled by the Larmor radius. On substantially larger length scales, such as concern us in this paper, field-line coupling is dominated by equation (3).

Below the top of the ionosphere (say, ~ 2000 km), the physics of the electric field involves ionization and recombination processes, as well as collisional conductivities in the E-region (where most of the ionospheric current associated with auroras is flowing). We have not considered the physics of this region in any detail, mostly because it is very complicated. To achieve the phenomenological approach used here, we need only note that

ionospheric return currents are generated in the collisional E-region, and that Poisson's equation allows us to relate $E_\parallel$ in this region to that in the magnetosphere. In the usual way, we express an ignorance of the detailed processes going on between the E-region and 2000 km by integrating over this range of altitude, as in (1) and (3). In this paper where there is no need to distinguish the E-region from the rest of the ionosphere, we adopt the convenient (but inprecise) terminology of referring to quantities with subscript ℓ as ionospheric. When there is need for a precise distinction, we use the subscript I to denote the E-region ionospere and ℓ for quantities evaluated at 2000 km (the baropause).

In using equations (3) and (4) we assume all quantities depend only on the coordinate x, the horizontal distance in the north-south direction at the baropause ($s=\ell$, where s is the distance along the field line from the equator). Of course, the magnetospheric potential ϕ_0 is originally given as a function of latitudinal distance at the equator x_E; they are related by $x = x_E (B_0/B_\ell)^{1/2}$, and $\phi_0 = \phi_0[x(B_\ell/B_0)^{1/2}]$. This means that when we speak of magnetospheric perpendicular electric fields, these fields are scaled geometrically to the ionosphere as if there were no parallel potential drop.

Originally equation (3) was derived for the case when the ionospheric potential $\phi(x)$ was greater than the magnetospheric potential $\phi_0(x)$ on a given field line, for only then could the relation $-J_\parallel \propto \phi-\phi_0$ be derived. ($J_\parallel < 0$ corresponds to downgoing electrons.) The reason is that the derivation of this relation depends on the smallness of the inverse mirror ratio (B_0/B_ℓ); this ratio enters because the distribution function of the precipitating electrons is originally specified at the equator, but evaluated at the ionosphere. A similar argument is not directly applicable to the return current, which has its source in the ionosphere. But other arguments, given below,

allow us to conclude that $-J_{\parallel}$ is still linear in $\phi-\phi_0$, even when this potential drop is reversed in sign, although the (positive) factors of proportionality are not necessarily the same for upgoing and downgoing $J_{\parallel}$. We thus generalize the current-potential relation to

$$-J_{\parallel} = Q(x)\ [\phi(x) - \phi_0(x)] \tag{5}$$

throughout the whole auroral region and for both signs of current; $Q > 0$ may depend on x both implicitly and explicitly, e.g., Q may assume different values for $\phi - \phi_0 > 0$ and for $\phi - \phi_0 < 0$.

It is actually a question of some delicacy whether, in (5), $\phi - \phi_0$ means $\phi_\ell - \phi_0$ or $\phi_I - \phi_0$. In contrast, this is not at issue for the same relation (2) used in the precipitation region, because $\phi_0 - \phi_\ell$ is much larger than $\phi_\ell - \phi_I$, that is, $\phi_0 - \phi_\ell \approx \phi_0 - \phi_I$ for the upward current region of electron precipitation. This is not so for the return current region, and exactly what we mean by $\phi - \phi_0$ in (5) affects the value of Q. Since we do not know very well what Q is in the return current region we leave this question open in our parametric studies of (5).

The return current, frequently observed to lie adjacent to the upward current of auroras [e.g., Kamide et al., 1979], is formed by conversion of directly-precipitating electrons, and their secondaries, into horizontal Pedersen current at altitudes $\lesssim$ 170 km (above 200 km, the Pedersen conductivity drops rapidly). These Pedersen currents carry a net negative charge to the edges of the precipitation region, which thus acquires a potential suitable for expelling ionospheric electrons upward along the magnetic field. (There are not enough magnetospheric ions to support the alternate scenario of ion precipitation [Lui et al., 1977].) The actual charge imbalance is very small,

only a tiny fraction of the charge carried in by precipitation. For example, a downward electron flux F, if not removed from the ionosphere promptly by return currents, produces a surface charge density at the ionosphere. The associated electric field produced by F over a time t is given by $E_\parallel = 4\pi eFt$. If $F = 10^9 e/cm^2 sec$, $t = 1$ sec, we find $E_\parallel \approx 200$ kV/m! Since in fact $E_\parallel$ is considerably less than 1 mV/m at the ionosphere, the net charge density of the ionosphere is less than 5 e/cm^2. Although this is a tiny charge imbalance, it is directly responsible for the return current flow. In our calculations we need not deal directly with the net charge density; it is clearly adequate to insist on current conservation, so that all the charge that flows into the ionosphere flows out again. Note that this condition is violated in Lyons' (1980, 1981) calculations.

Now we must relate the return current density to the electric field produced by the charge imbalance of the ionosphere. Since the return current is created in the collisional E-region, the relation between current and field is the usual one: $J_\parallel = \sigma_\parallel E_\parallel$. Actually, this should be integrated over the various altitudes at which conversion of Pedersen current to field-aligned current takes place; we do not know the details of this process, so instead we employ height-integrated quantities:

$$J_\parallel = \frac{Ne^2}{m \nu_\parallel h} (\phi_I - \phi_\ell) \qquad (6)$$

Here $\nu_\parallel$ is an effective height-averaged collision frequency, and h is the altitude difference between the collisional ionosphere and the regime where collisions are ineffective (roughly the baropause). Above the baropause, $J_\parallel$ is given by a geometric scaling law expressing the opening-up of flux tubes:

$$s < \ell: \quad J_{\parallel}(s) = J_{\parallel}(\ell) \frac{B(s)}{B_{\ell}} \tag{7}$$

Furthermore, for $s < \ell$, $E_{\parallel}(s)$ is given by the same scaling as in (7). To see this, return to Poisson's equation (4), averaged over a horizontal distance Δx larger than the ion Larmor radius (a few km), but small compared to the size of the return current region (50-100 km). The first term on the left of (4) is small after averaging, and we drop it. The charge density (right-hand side of (4)) is likewise small, since magnetic mirror forces do not act to separate the low-energy electrons and ions. One then concludes that

$$s < \ell: \quad E_{\parallel}(s) = E_{\parallel}(\ell) \frac{B(s)}{B_{\ell}} \sim \frac{(\phi_I - \phi_{\ell})}{h} \frac{B(s)}{B_{\ell}} \tag{8}$$

in the return current region. Of course, (6) - (8) together tell us that $J_{\parallel} \sim (\phi_I - \phi_{\ell})$ <u>everywhere</u> along the line, while (8) can be integrated over s from 0 to ℓ to give $(\phi_0 - \phi_{\ell})$ as varying linearly with $\phi_I - \phi_{\ell}$. Then (5), the proportionality of current to $\phi - \phi_0$, is established for the return current region. As we have said, the constant of proportionality depends on whether by ϕ we mean ϕ_I or ϕ_{ℓ}.

In summary, the "mapping" of a given magnetospheric potential distribution $\phi_0(x)$ to the ionospheric E-region (where the potential distribution is $\phi(x)$) in the presence of field-aligned potential drop distribution $\phi(x) - \phi_0(x)$ is governed by

$$\frac{d}{dx} F(x) \frac{d\phi}{dx} = \kappa^2(x) [\phi(x) - \phi_0(x)] \tag{9}$$

where F is the dimensionless profile of the height-integrated ionospheric Pedersen conductivity $\Sigma_p(x) \equiv \Sigma_0 F(x)$ such that $F(\pm\infty)=1$. The function $\kappa(x) \equiv$

$[Q(x)/\Sigma_0]^{1/2} > 0$ is an inverse scale length set by the magnetosphere-ionosphere coupling. From (9), it is clear that this natural scale acts as a filter as the distribution $\phi_0(x)$ is "mapped" into $\phi(x)$. The solution of (9) under various physical restraints, such as (4), will be the main topic to be dealt with in this paper.

We have already said that the ionosphere is slightly charged, but by an extremely tiny amount (the precipitated charge is relieved by the return current). Equally negligible is the net charge of the magnetosphere-ionosphere system, integrated for $x = -\infty$ to ∞. It thus follows from Poisson's equation (4), integrated over all x with neglect of the right-hand side, that

$$E_\perp(\infty) - E_\perp(-\infty) = 0 = \phi'(-\infty) - \phi'(\infty) \tag{10}$$

By integrating (4) from $-\infty$ to ∞, we learn that

$$\int_{-\infty}^{\infty} dx\, \kappa^2(x)\, [\phi(x) - \phi_0(x)] = \phi'(\infty) - \phi'(-\infty) = 0 \tag{11}$$

This shows immediately that $\phi(x) - \phi_0(x)$ must change sign; the crossover point x_c, where $\phi(x_c) = \phi_0(x_c)$, is the boundary between the region of direct electron precipitation and the return current.

III. GENERAL FEATURES OF ELECTRIC FIELD MAPPING

As has been alluded to previously, a major purpose of this paper is to analyze the dependence of the ionospheric electric potential response upon the imposed magnetospheric dynamo potential distribution and upon the boundary and charge constraint conditions assumed. For purposes of establishing the consistency of boundary values for the general scheme formulated by Chiu and Cornwall [1980], it is convenient to consider the case of constant (but discontinuous) parameters F and κ in (9). On the practical side, since the entire problem with constant parameters can be solved analytically, the results of this section provide the basis for analysis without the encumbrances of a computational effort. We shall show in the next section that our conclusions are not basically altered when F and κ are made functions of x.

For constant parameters (F = 1, κ = constant) in (9), the general solution can be written as

$$\phi(x) = Ce^{-\kappa x} + De^{+\kappa x} + \frac{\kappa}{2}\int^{x} dy\ \phi_0(y)\ e^{-\kappa(x-y)} + \frac{\kappa}{2}\int_{x} dy\ \phi_0(y)e^{\kappa(x-y)} \quad (13)$$

where the determination of constants (C, D) and the integration limits depend on boundary conditions. Note that (13) is written in terms of the general one-dimensional Green's function solution for given source function ϕ_0; hence, the interpretation that ϕ is the ionospheric response to ϕ_0. Because $\kappa = [Q/\Sigma_0]^{1/2}$ can be different constants in the upward and downward current regions, the complete solution for ϕ with a given set of values of κ, must be made continuous at the boundary of the two regions; indeed, this procedure can be applied for any number of regions of different κ values.

As an example, let us consider the explicit solution specified by the following conditions:

a. The ionospheric potential $\phi(x)$ and the dynamo potential $\phi_0(x)$ are symmetric about the origin; thus $\phi(x) = \phi(-x)$, so we need only consider the domain $0 \leq x < \infty$.

b. The domain $0 \leq x < \infty$ is split into two regions defined by different constant values of F and κ. Because these parameters are assumed constant, we can set F = 1 and (9) is specified by a single parameter κ_i (i = 1, 2) in each region. The boundary between the two regions is labeled $x = x_c$. Thus, (9) becomes

$$\phi''_{1,2} = \kappa^2_{1,2} (\phi_{1,2} - \phi_0) \tag{14}$$

with $0 \leq x \leq x_c$ labeled as region 1 and $x_c \leq x < \infty$ labeled as region 2.

c. The total integrated charge of the ionosphere is assumed zero. The symmetry assumption a above implies that total charge in $0 \leq x < \infty$ also vanishes, as expressed in (10). Adopting the notation of that equation, we have

$$\phi'_2(\infty) - \phi'_1(0) = 0 \tag{15}$$

Now because of the symmetry assumption, $\phi_1(0)$ must be an extremum, i.e., $\phi'_1(0) = 0$. Therefore, the effects of assumptions a, b and c correspond to the boundary conditions

$$\phi'_1(0) = \phi'_2(\infty) = 0 \tag{16}$$

d. At the interface $x = x_c$, we require the continuity of ϕ and its derivative (a discontinuity in ϕ' would imply a surface charge layer at x_c):

$$\phi_1(x_c) = \phi_2(x_c) \tag{17}$$

$$\phi_1'(x_c) = \phi_2'(x_c) \tag{18}$$

Up to this point, we have treated the interfacial point $x = x_c$ as if given; but, by virtue of its definition as the interface between regions of upward and downward current, we have by application of (5) at x_c

$$\phi_0(x_c) = \phi_1(x_c) = \phi_2(x_c) \tag{19}$$

where the second equality of (19) is redundant with (17). In addition to the four boundary conditions (16) - (18), which determine the set of four coefficients, (C_1, C_2, D_1, D_2) in terms of x_c, (19) is a transcendental equation for x_c. To render the procedure more explicit, we write the regional solutions to (14)

$$\phi_1(x) = C_1 e^{-\kappa_1 x} + D_1 e^{\kappa_1 x} + \frac{\kappa_1}{2}\int_0^x dy\ \phi_0(y) e^{\kappa_1(y-x)} - \frac{\kappa_1}{2}\int_0^x dy\ \phi_0(y) e^{-\kappa_1(y-x)} \tag{20}$$

$$\phi_2(x) = C_2 e^{-\kappa_2 x} + \frac{\kappa_2}{2}\int_{x_c}^x dy\ \phi_0(y) e^{\kappa_2(y-x)} + \frac{\kappa_2}{2}\int_x^\infty dy\ \phi_0(y) e^{-\kappa_2(y-x)} \tag{21}$$

from which (16) - (19) can be applied to determine the unknown constants in terms of the parameters κ_1 and κ_2. The procedure is straightforward for an assumed $\phi_0(x)$.

As an example, we show in Fig. 1 a solution ϕ for a given ϕ_0 of the form

$$\phi_0(x) = A\,[e^{-ax} - (a/b)\,e^{-bx}] \tag{22}$$

where $a^{-1} = 76.5$ km, $b^{-1} = 73.5$ km and A is a normalization so chosen that $\phi_0(0) = A(1-a/b) < 0$ is equivalent to ten divisions of the ordinate of Fig. 2. The scale length of ϕ_0 is (because a is nearly equal to b) about 160 km; whereas the natural scale lengths κ_1^{-1} and κ_2^{-1} are respectively 75 km and 53 km. From Fig. 2, the distance x_c to the cross-over point is about 160 km, while the return current extends for some distance past that.

It is clear from (20) and (21) that the scale length associated with the ionospheric potential $\phi(x)$ depends on the κ_1 as well as on the scale associated with ϕ_0. This correlation of scales is analogous to electric field mapping in the collisional ionosphere (Chiu, 1974), where finite but different parallel and perpendicular conductivities play the same roles as our field-aligned and Pedersen currents. As in the case of ionospheric electric field mapping, 't would be convenient to have a "rule of thumb" for the convolution of scales of the potential drop. For this prupose, we consider the case of a dynamo potential of scale γ^{-1}:

$$\phi_0(x) = Ae^{-\gamma x} \tag{23}$$

in the simplest situation in which $\kappa_1 = \kappa_2 = \kappa$. This ϕ_0 has a discontinuity in $E_{\perp 0}(x)$ at $x = 0$, which makes it somewhat artificial.

An easy calculation yields the cross-over distance x_c:

$$x_c = (\gamma-\kappa)^{-1}\,\ell n\,(\gamma/\kappa) \tag{24a}$$

If, instead of taking $\kappa_1 = \kappa_2 = \kappa$, we take $\kappa_1 = \kappa$, $\kappa_2 = \infty$ (which forces $\phi(x) = \phi_0(x)$for $x > x_c$), x_c is increased by a factor of two over the value given by (24a). The opposite extreme of $\kappa_2 = 0$ yields scale lengths in the range 1.4-2 times x_c in (24a), depending on γ/κ. That is to say x_c varies by at most a factor of two when κ_2 is varied.

An important scale length is that of the potential difference $\phi - \phi_0$, since it is a measurable quantity. From (13) and (23) we find this scale length to be

$$x_d^{-1} \equiv -\frac{d}{dx} \ln(\phi-\phi_0) = \kappa - \frac{\gamma^2}{(\gamma + \kappa)} \frac{\phi_0}{\phi - \phi_0} \tag{24b}$$

Note that as $\gamma \to 0$ the cross-over distance x_c approaches infinity, while $x_d \to \kappa^{-1}$; this is the case considered by Lyons (1980). (In later work, Lyons (1981) has considered finite γ.) In our simple example x_c is independent of potentials, but x_d depends on them. We estimate at x=0 that $-\phi_0(\phi-\phi_0)^{-1}$ lies between 1 and 3 for typical cases, so (24) shows that x_d is governed by γ^{-1} in the limit of large γ, but tends to κ^{-1} for small γ. That is, small-scale magnetospheric structure can be transmitted down to the ionosphere with little change, but if the magnetospheric scale length (of course, mapped geomatrically onto the ionosphere) is large compared to κ^{-1}, the scale length of the inverted-V region tends to κ^{-1}. It is important that small-scale magnetospheric structures are not filtered out, since they may well be responsible for small-scale (in Lamor radius) effects observed in the auroral ionosphere [e.g., Swift, 1979; Lysak and Carlson, 1981].

Now we come to one of the most important features of equation (14) and its associated boundary conditions: The central potential drop $\Delta\phi \equiv \phi(0)-$

$\phi_0(0)$ is <u>not</u> an undetermined parameter; instead it is set by the scale length κ and by the magnetospheric $E_{\perp 0}(x)$, geometrically mapped onto the ionosphere. This means that the large-scale convection field mapping problem can be solved with relatively minor modifications to the solution for zero parallel potential drop. It is not our purpose to discuss this large-scale mapping in detail here, so we simplify to the case of constant κ to make our point. It is then an easy matter to integrate (20) by parts and find:

$$\Delta\phi \equiv \phi(0) - \phi_0(0) = -\int_0^\infty dx\, e^{-\kappa x} E_{\perp 0}(x) \tag{25}$$

(Of course, appropriate values for C and D are used, which satisfy the boundary conditions of symmetry around $x = 0$ and vanishing fields at $x = \infty$.) One may estimate $\Delta\phi$ from (25) by assuming, e.g., $-E_{\perp 0}(x) \approx 100$ mV/m and $\kappa^{-1} \approx 50$ km which gives $\Delta\phi \approx 5$ kV; this nominal value will decrease if $E_{\perp 0}$ decreases with x (as, for example, in (23)).

We see that $\Delta\phi$ is determined in part by properties of magnetospheric particles through κ (see the discussion below equation (2)), in part by ionospheric current conservation which couples neighboring field lines together, and in part by perpendicular magnetospheric electric fields. If any of these ingredients is left out, it is not possible to determine the central potential drop $\Delta\phi$. Conversely, we can also say that $\Delta\phi \neq 0$ is the result of all these ingredients put together.

IV. SPECIFIC EXAMPLES OF ELECTRIC FIELD MAPPING

As we have indicated in the previous section, our model suggests that the magnitudes of the height-integrated Pedersen conductivity, Σ_p, and the parallel current density, $J_\parallel$, directly affect the length scale associated with the mapped electrostatic potential in the ionosphere. In this section we investigate more closely the sensitivity of this mapping to latitudinal variations of these parameters perpendicular to the magnetic field.

In the absence of conclusive observational descriptions of the spatial variation of Σ_p, and $J_\parallel$; we have considered three kinds of variability which should bracket the physical characteristics we wish to model. Solutions to (9) are discussed for three different assumptions: 1) F and κ are spatially constant; 2) F and κ assume constant values but κ experiences a discontinuous jump between regions of upgoing and downgoing current; 3) κ is constant, but F decreases exponetially as one goes from the precipitation region to the return-current region (that is, Σ_p is enhanced in the precipitation region). Of course, case 1) was discussed extensively in the last section.

Case 2) was also discussed briefly, in the special example of an exponential ϕ_0. A somewhat more realistic ϕ_0 is that used for Fig. 2, and given in (22); it has no discontinuity in $E_{\perp 0}(x)$ at $x=0$. Fig. 3 shows the results of numerical integration of (14) for different κ_1/κ_2, with κ_1^{-1} fixed at 75 km. The most obvious result is a strong variation in the average return-current potential drop, as necessitated by current conservation (the return current varies as $\kappa_2^2(\phi - \phi_0)$, so a smaller κ_2 requires a larger potential drop). For $\kappa_2^2 = 10\kappa_1^2$ the return-current potential drop is 25 times smaller than the central potential drop, and 5 times smaller for $\kappa_2 = \kappa_1$. Note from Fig. 3 that

the central potential drop increases slightly as κ_2 increases, and that x_c does not move very much.

So far, we have studiously avoided estimating the value of κ_2 (that is, Q in the return-current region). This is because κ_2 is not easy to estimate reliably, since it depends on quantities which vary significantly with altitude in the ionosphere. But the reader is entitled to some feeling for the ratio κ_2/κ_1, so we offer the following estimate. From Chiu and Cornwall [1980], we recall

$$|J^1_{\parallel \ell}| = N_{M-}\, e(2 + \frac{A_2}{3})(e|\Delta\phi^1_\ell|/kT_{\perp-})(kT_{\parallel-}/2\pi m_e)^{1/2} \tag{26}$$

From (6), we have

$$|J^2_{\parallel \ell}| = N_{I-}\, e^2\, |\Delta\phi^2_\ell|/m_e\, h\, \nu_\parallel \tag{27}$$

In (26) and (27), superscripts 1 and 2 refer to upward and downward currents, respectively. The ratio of currents is thus

$$|J^1_{\parallel \ell}|/|J^2_{\parallel \ell}| = \frac{(2+A_2/3)}{(2\pi)^{1/2}} (\frac{N_{M-}}{N_{I-}})(\frac{m_e\, T_{\parallel-}}{k\, T^2_{\perp-}})^{1/2} h\nu_\parallel \cdot \frac{|\Delta\phi^1_\ell|}{|\Delta\phi^2_\ell|} \tag{28}$$

Applying case W of Chiu and Schulz [1978] to (28), one has the magnetospheric parameters: $kT_{\parallel-} = 0.189$ keV, $kT_{\perp-} = 0.775$ keV, $N_{M-} = 3$ cm^{-3}. For ionospheric parameters, the lumped quantity $h\nu_\parallel/N_{I-} \sim 10^3$ cm^2/sec for nighttime conditions is used to obtain

$$|J^1_{\parallel \ell}|/|J^2_{\parallel \ell}| \approx 0.2\, |\Delta\phi^1_\ell|/|\Delta\phi^2_\ell| \tag{29}$$

If taken seriously, this indicates that $Q_1/Q_2 = 0.2$. In view of the fact that Σ_1/Σ_2 is likely to be greater than one (because of precipitation enhancement), it is likely that $\kappa_2^2/\kappa_1^2 = (Q_2/Q_1)(\Sigma_1/\Sigma_2)$ is at least 10 and possibly larger. This means (see Fig. 3) that return-current electrons have energies of 100 eV or less.

Turn now to case 3), where the precipitation enhancement of Σ_p is modeled by an exponential, varying from 10 mho at x=0 to 1 mho at large x. We have fixed $\kappa_1^{-1} = \kappa_2^{-1} = 80$ km, and, as shown in Fig. 4, take the conductivity scale length to be either κ^{-1} or $0.5\ \kappa^{-1}$ (also shown for comparison is the case $\Sigma_p = 5$ mho everywhere). The dynamo potential ϕ_0 is the same as for Figs. 2 and 3 (see equation (22)). The general features associated with the earlier figures persist: The cross-over point x_c does not change much, and the return-current potential drop is significantly less than the central potential drop. The more rapid the falloff of Σ_p, the larger this ratio of potential drops becomes.

V. ELECTROSTATIC POTENTIAL TOPOLOGIES: S AND V SHAPES

So far, we have only considered potentials ϕ and ϕ_0 which are symmetric about x=0, with antisymmetric electric fields. This presumably is associated with the classic inverted-V structure seen in auroral electron measurements [Frank and Ackerson, 1971, 1972; Gurnett, 1972; Mizera et al., 1976; Mizera and Fennell, 1977]. But it has been suggested that asymmetric potential structures (called S-shapes) may happen even more frequently than V-shapes. V-shaped equipotential contours are always associated with $E_\perp$ reversals, as shown in Fig. 5. Whereas, the term "S-shape" refers to equipotential contours which deviate from field lines, but do not show $E_\perp$ reversals. Fig. 5 makes it clear that every V-shaped (or symmetric) potential has S-shaped equipotential contours on its wings. A satellite crossing this symmetric potential structure at any altitude can detect a V-shaped region.

But this is not the only possibility in principle. There can be asymmetric potential structures which look V-shaped at sufficiently high altitudes, but are only S-shaped at lower altitudes. An example is shown in Fig. 6, in which the region of negative x has equipotential field lines, with an auroral structure for $x > 0$. We do not know why the situation of Fig. 6 should occur with any particular frequency, compared to the occurrence of more or less symmetric potentials, but experimenters should keep in mind the possibility that low-altitude electric field measurements might show a different topology than seen on high-altitude satellites. It will be interesting to see what the Dynamics Explorer satellites see in this regard.

VI. CONCLUSIONS

1. We have extended the differential equation used in an earlier work [Chiu and Cornwall, 1980] to encompass the return-current region. This requires knowledge of the proportionality factor between $-J_{\parallel}$ and $\phi - \phi_0$, which we can estimate only crudely at the moment. (That $J_{\parallel}$ is proportional to $\phi - \phi_0$ is really nothing but Ohm's law, which is applicable to the return current because it is generated in the collisional ionosphere.) These estimates suggest that the return current, contiguous to and just outside the region of auroral precipitation, is carried by electrons of 100 eV or less. The cross-over point between upward and downward current is 100-150 km from the center of the inverted-V, for a wide variety of auroral parameters. An essential ingredient of this extended equation is the boundary condition of no net current flow in or out of the ionosphere, so that the ionosphere is not charged to grossly unphysical values. The ionosphere carries an extremely small negative charge which is responsible for driving the return current.

2. Our differential equation couples neighboring field lines to each other. As a result, it is not possible to assign parallel potential drops more or less arbitrarily, as earlier workers who did not consider ionospheric current conservations were forced to do. The total parallel potential drop along the center field line of an aurora is uniquely determined by perpendicular magnetospheric electric fields, convolved with a Green's function which has a scale length κ^{-1} determined by both ionospheric parameters and by the number and momentum of auroral primaries: $\kappa^2 = Q/\Sigma_p$, $Q = Ne^2/M\bar{\nu}$. This unique determination of parallel potentials means that the problem of constructing $\vec{E}$ (both $E_{\perp}$ and $E_{\parallel}$) everywhere in the magnetosphere, given $E_{\perp}$ on a boundary surface can be solved straightforwardly (in principle, at least).

3. The Green's function integrals which solve our differential equation show that small-scale structures in $E_{\perp 0}(x)$, the equatorial magnetospheric field, are mapped onto the ionosphere. But large-scale structure is hidden, and the overall ionospheric scale size of inverted-V auroras is $\kappa^{-1} \approx 100$ km. So κ^{-1} may be called the outer scale size of inverted V's. There is, of course, much small-scale structure in auroral arcs, and many authors believe that it is mapped down from small-scale structures created near the equator of auroral field lines.

4. Different boundary conditions imposed on the differential equation yield topologically-distinct solutions. Latitudinal symmetry about a center line implies equipotential contours with a V shape at all altitudes (sufficiently close to the center line). Asymmetric boundary conditions can push the V-shaped region to a finite altitude, leaving only S-shaped potentials below. The Dynamics Explorer satellites will, we hope, settle this question of the nature of V-shapes and S-shapes.

APPENDIX

In this Appendix we show that the kinetic Ohm's law (2) holds for arbitrary electron distribution function.

Let $\epsilon_\parallel \equiv v_{\parallel 0}^2$ and $\epsilon_\perp \equiv v_{\perp 0}^2$ be the constants of motion for an electron moving on a magnetic field line; these are related to the local velocities at any point s on the line by

$$v_{\parallel 0}^2 = v_\parallel^2 + v_\perp^2 \left(1 - \frac{B_0}{B(s)}\right) - \frac{2e}{M} \left(\phi(s) - \phi_0\right) \tag{A-1}$$

$$v_{\perp 0}^2 = \frac{B_0}{B(s)} \; v_\perp^2 \tag{A-2}$$

The equatorial distribution function ($s=0$, $B=B_0$, $\phi=\phi_0$) is $f(\epsilon_\parallel, \epsilon_\perp)$.

We are interested in the current at the ionosphere ($s=\ell$) produced by electrons arriving there from the equator. The velocity-space integral which defines $J_\parallel$ is subject to the constraints

$$v_\parallel > 0, \; v_\parallel^2 > 0 \tag{A-3}$$

which translates to the constraints

$$\frac{-J_\parallel}{N_e} = 2\pi \int_0^\infty v_\perp \, dv_\perp \int_0^\infty v_\parallel \, dv_\parallel \, f =$$

$$= \frac{\pi}{2} \left(\frac{B_\ell}{B_0}\right) \int_0^\infty d\epsilon_\perp \int_0^\infty d\epsilon_\parallel \, f(\epsilon_\parallel, \epsilon_\perp) \left\{\theta(R-\epsilon_\perp) + \right.$$

$$\left. + \theta(\epsilon_\perp - R) \, \theta\left[\epsilon_\parallel - \left(\frac{B_\ell - B_0}{B_0}\right) (\epsilon_\perp - R)\right]\right\} \tag{A-4}$$

where θ is the usual step function and

$$R = \frac{2e}{M} \left(\frac{B_0}{B_\ell - B_0}\right) (\phi_\ell - \phi_0) > 0 \qquad \text{(A-5)}$$

Now $B_0/B_\ell \ll 1$ so that if, as we assume, the average value of $\varepsilon_\perp$ is not large compared to (e/M) $(\phi_\ell - \phi_0)$, we can replace $\varepsilon_\perp$ by 0 in f for the terms $\theta(R-\varepsilon_\perp)$ in (A-4). Likewise in the second θ-function in (A-4) we can set R=0, so $0 \leq \varepsilon_\perp \leq (B_0/B_\ell)\ \varepsilon_\parallel = o$. It is then straightforward to find

$$\frac{-J_\parallel}{N_e} = \frac{\pi}{2} \int_0^\infty d\varepsilon_\parallel\ f(\varepsilon_\parallel, 0)[\varepsilon_\parallel + \frac{2e}{M} (\phi_\ell - \phi_0)] + O(B_0/B_\ell) \qquad \text{(A-6)}$$

The $\varepsilon_\parallel$ term in square brackets represents the diffuse auroral current (leakage into the loss cone), and will be neglected in this work. The second term gives rise to equation (2), where comparison with (A-6) shows that $Q = N_e^2/M\bar{v}$ where $\bar{v}$ is a typical velocity for f.

Acknowledgment

The authors acknowledge beneficial discussions on various aspects of this paper with S. -I. Akasofu, D. S. Evans, J. F. Fennell, D. J. Gorney, M. K. Hudson, J. R. Kan, J. Lemaire, L. R. Lyons, R. L. Lysak, P. F. Mizera, M. Schulz and R. R. Vondrak.

REFERENCES

Chiu, Y. T., Self-consistent electrostatic field mapping in the high-latitude ionosphere, J. Geophys. Res., 79, 2790 (1974).

Chiu, Y. T. and J. M. Cornwall, Electrostatic model of a quiet auroral arc, J. Geophys. Res., 85, 543 (1980).

Chiu, Y. T. and M. Schulz, Self-consistent particle and parallel electrostatic field distributions in the magnetospheric-ionospheric auroral region, J. Geophys. Res., 83, 629 (1978).

Chiu, Y. T., J. M. Cornwall and M. Schulz, Auroral magnetosphere-ionosphere coupling: a brief topical review, Solar Terrestrial Proceedings, ed. R. F. Donnelly, Vol. 2, p. 494, NOAA, Boulder, Colo. (1980).

Chiu, Y. T., J. M. Cornwall and M. Schulz, Effects of auroral-particle anisotropies and mirror forces on high-latitude electric fields, invited paper, Chapman Conference on Formation of Auroral Arcs, Fairbanks, Alaska 21-24 July, 1980. To be published in AGU monograph, ed. S. -I. Akasofu, (1981).

Croley, D. R., Jr., P. F. Mizera and J. F. Fennell, Signature of a parallel electric field in ion and electron distributions in velocity space, J. Geophys. Res., 83, 2701 (1978).

Evans, D. S., Precipitating electron fluxes formed by a magnetic field-aligned potential difference, J. Geophys. Res., 79, 2853 (1974).

Frank, L. A. and K. L. Ackerson, Observation of charged particle precipitation into the auroral zone, J. Geophys. Res., 76, 3612 (1971).

Fridman, M. and J. Lemaire, Relationship between auroral electron fluxes and field-aligned electric potential difference, J. Geophys. Res., 85, 664

(1980).

Geortz, C. K. and R. W. Boswell, Magnetospheric-ionospheric coupling, J. Geophys. Res., 84, 7239 (1979).

Gurnett, D. A. and L. A. Frank, Observed relationships between electric fields and auroral particle precipitation, J. Geophys. Res., 78, 145 (1973).

Hudson, M. K. and F. S. Mozer, Electrostatic shocks, double layers and anomalous resistivity in the magnetosphere, Geophys. Res. Lett., 5, 131 (1978).

Kamide, Y., J. S. Murphree, C. D. Anger, F. T. Berkey and T. A. Potemra, Nearly simultaneous observations of field-aligned currents and visible auroras by the Triad and Isis 2 satellites, J. Geophys. Res., 84, 4425 (1979).

Kan, J. R., Energization of auroral electrons by electrostatic shock waves, J. Geophys. Res., 80, 2089 (1975).

Kan, J. R. and L. C. Lee, Theory of imperfect magnetosphere-ionosphere coupling, Geophys. Res. Lett., 7, 633 (1980).

Lemaire, J. and M. Scherer, Ionosphere-plasmasheet field-aligned currents and parallel electric fields, Planet. Space Sci., 22, 1485 (1974).

Lui, A. T. Y., D. Venkatesan, C. D. Anger, S. -I. Akasofu, W. J. Heikkila, J. D. Winningham and J. R. Burrows, Simultaneous observations of particle precipitations and auroral emissions by the Isis 2 satellite in the 19-24 MLT sector, J. Geophys. Res., 82, 2210 (1977).

Lyons, L. R., Generation of large-scale regions of auroral currents, electric potentials, and precipitation by the divergence of the convection electric field, J. Geophys. Res., 85, 17 (1980).

Lyons, L. R., Discrete aurora as the direct result of an inferred, high-altitude generating potential distribution, J. Geophys. Res., 86, 1

(1981).

Lyons, L. R., D. S. Evans and R. Lundin, An observed relation between magnetic field aligned electric fields and downward electron energy fluxes in the vicinity of the auroral forms, J. Geophys. Res., 84, 457 (1979).

Lysak, R. L. and C. W. Carlson, The effect of microscopic turbulence on magnetosphere-ionosphere coupling, Geophys. Res. Lett., accepted, 1981.

Miura, A. and T. Sato, Numerical simulation of global formation of auroral arcs, J. Geophys. Res., 85, 73 (1980).

Mizera, P. F. and J. F. Fennell, Signatures of electric fields from high and low altitude particle distributions, Geophys. Res. Lett., 4, 311 (1977).

Mozer, F. S., Electric field mapping in the ionosphere at the equatorial plane, Planet. Space Sci., 18, 259 (1970).

Mozer, F. S., Power spectra of the magnetospheric electric field, J. Geophys. Res., 76, 3651 (1970).

Mozer, F. S., C. W. Carlson, M. K. Hudson, R. B. Torbert, B. Paraday, J. Yatteau and M. C. Kelley, Observations of paired electrostatic shocks in the polar magnetosphere, Phys. Rev. Lett., 38, 292 (1977).

Sato, T., A theory of quiet auroral arcs, J. Geophys. Res., 83, 1042 (1978).

Shelley, E. G., R. D. Sharp and R. G. Johnson, Satellite observations of an ionospheric acceleration mechanism, Geophys. Res. Lett., 6, 54 (1976).

Stern, D. P., Quasi-neutral parallel electric fields, Rev. Geophys. Space Phys., accepted (1981).

Swift, D. W., On the formation of auroral arcs and acceleration of auroral electrons, J. Geophys. Res., 80, 2096 (1975).

Temerin, M., C. Cattell, R. Lysak, M. Hudson, R. Torbert, F. S. Mozer, R. D. Sharp, P. F. Mizera and P. M. Kintner, The small-scale structure of electrostatic shocks, J. Geophys. Res., submitted (1981).

Figure Captions

1. Electrostatic field mapping along field lines L_1 and L_2 between the magnetospheric equator (E_M) and the ionosphere (E_I) with or without a magnetic field-aligned potential drop $\Delta\phi_{MI}$.
2. Latitudinal structure of the electrostatic potential associated with the magnetospheric boundary, ϕ_0, and with the ionospheric boundary, ϕ. x_c is the position at which $\phi = \phi_0$.
3. Latitudinal structure of ϕ and ϕ_0 from (9) with $\kappa = \kappa_1$ for $x < x_c$ and $\kappa = \kappa_2 = \sqrt{m}\,\kappa_1$ for $x > x_c$. Variations in m allow different values of $J_\parallel$ in regions of upgoing and downgoing current (F = 1).
4. Latitudinal structure of ϕ and ϕ_0 for an exponentially varying integrated Pedersen conductivity, $\Sigma_p = 9.1e^{-m\kappa x} + 0.9$. ($\kappa = \kappa_1$ is kept constant.)
5. Interpolated equipotential structure from the geometrically mapped magnetospheric boundary to the ionosphere. Arrows indicate the direction of the electric field. Notations V and S indicate regions of V-shaped and S-shaped potential structure.
6. Same as Fig. 5 for a different imposed magnetospheric potential structure.

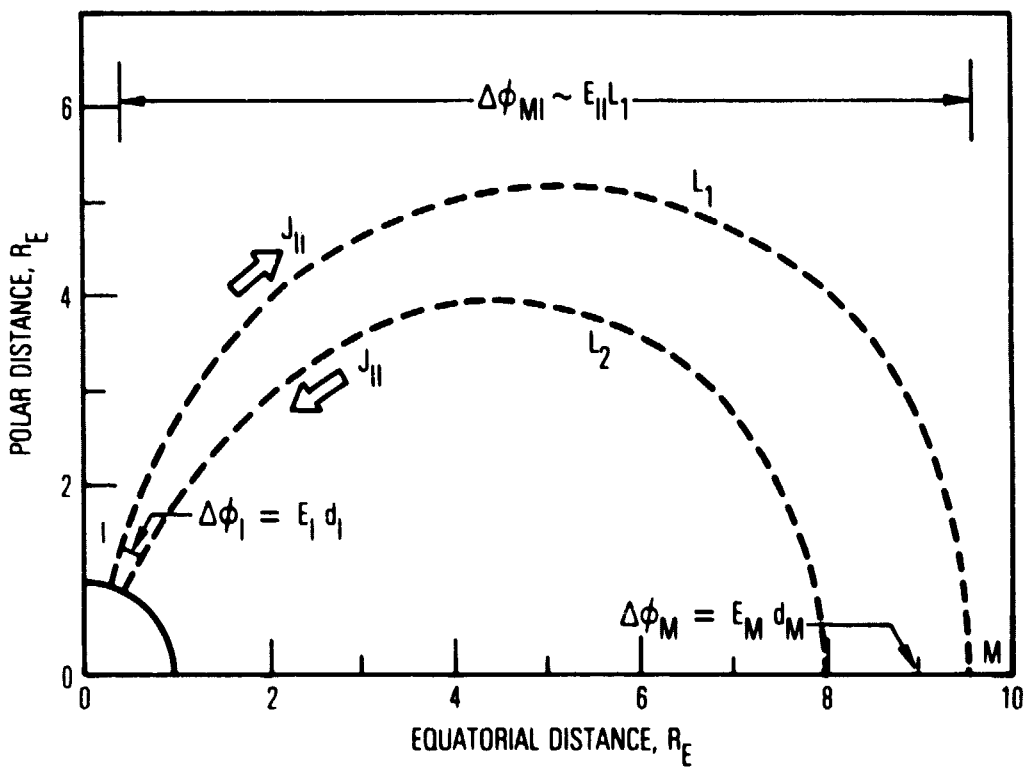
$\Delta\phi_{MI} \sim E_{II} L_1$
L_1
L_2
J_{II}
J_{II}
$\Delta\phi_I = E_I d_I$
$\Delta\phi_M = E_M d_M$
I
M
POLAR DISTANCE, R_E
EQUATORIAL DISTANCE, R_E
0
2
4
6
8
10

Fig. 1

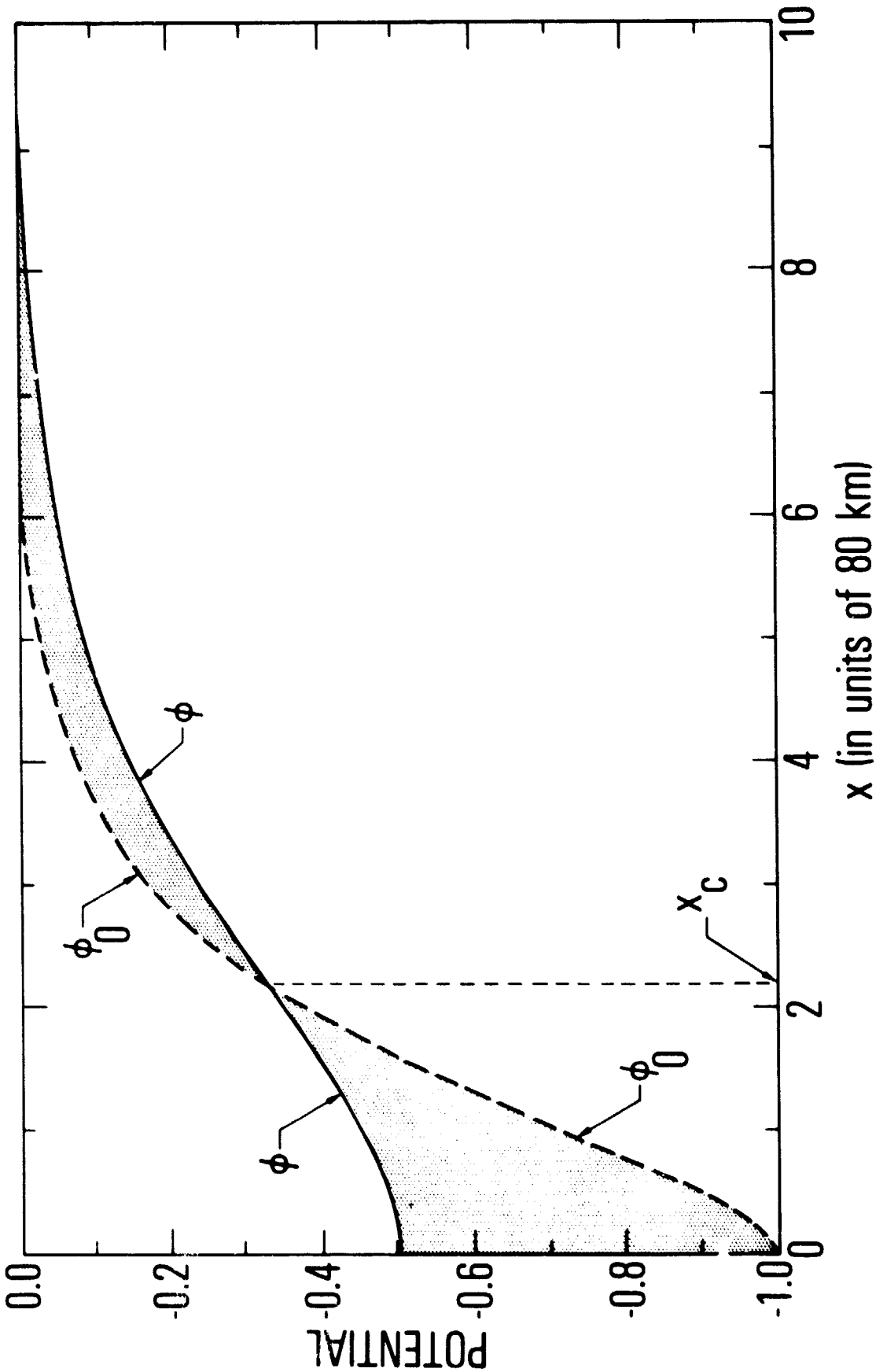
POTENTIAL
0.0
-0.2
-0.4
-0.6
-0.8
-1.0
0
2
4
6
8
10
x (in units of 80 km)
x_c
ϕ
ϕ_0
ϕ
ϕ_0

Fig. 2

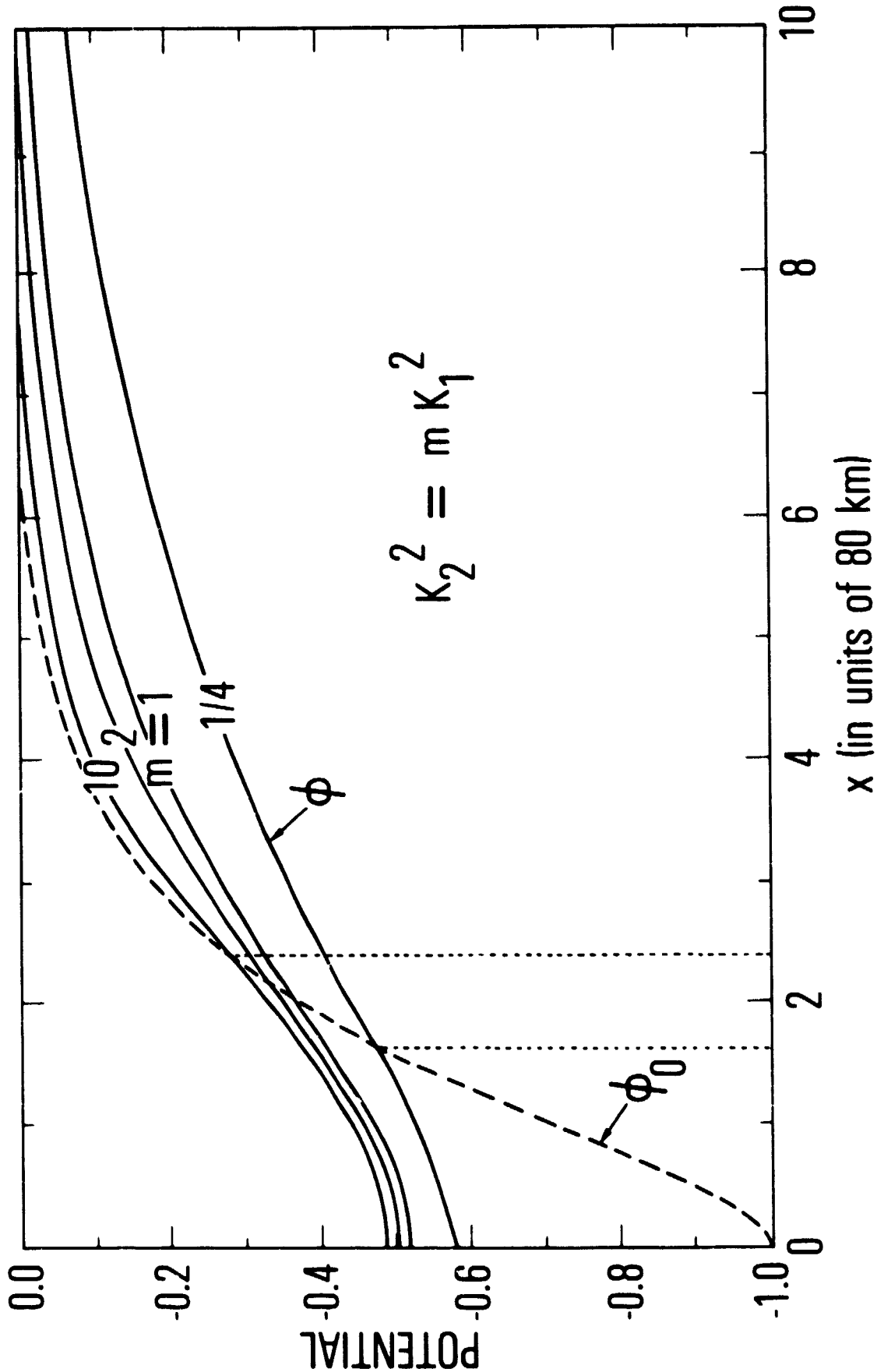
POTENTIAL
0.0
-0.2
-0.4
-0.6
-0.8
-1.0
0
2
4
6
8
10
x (in units of 80 km)
$K_2^2 = m K_1^2$
m = 1
1/4
2
10
ϕ
ϕ_0

Fig
3

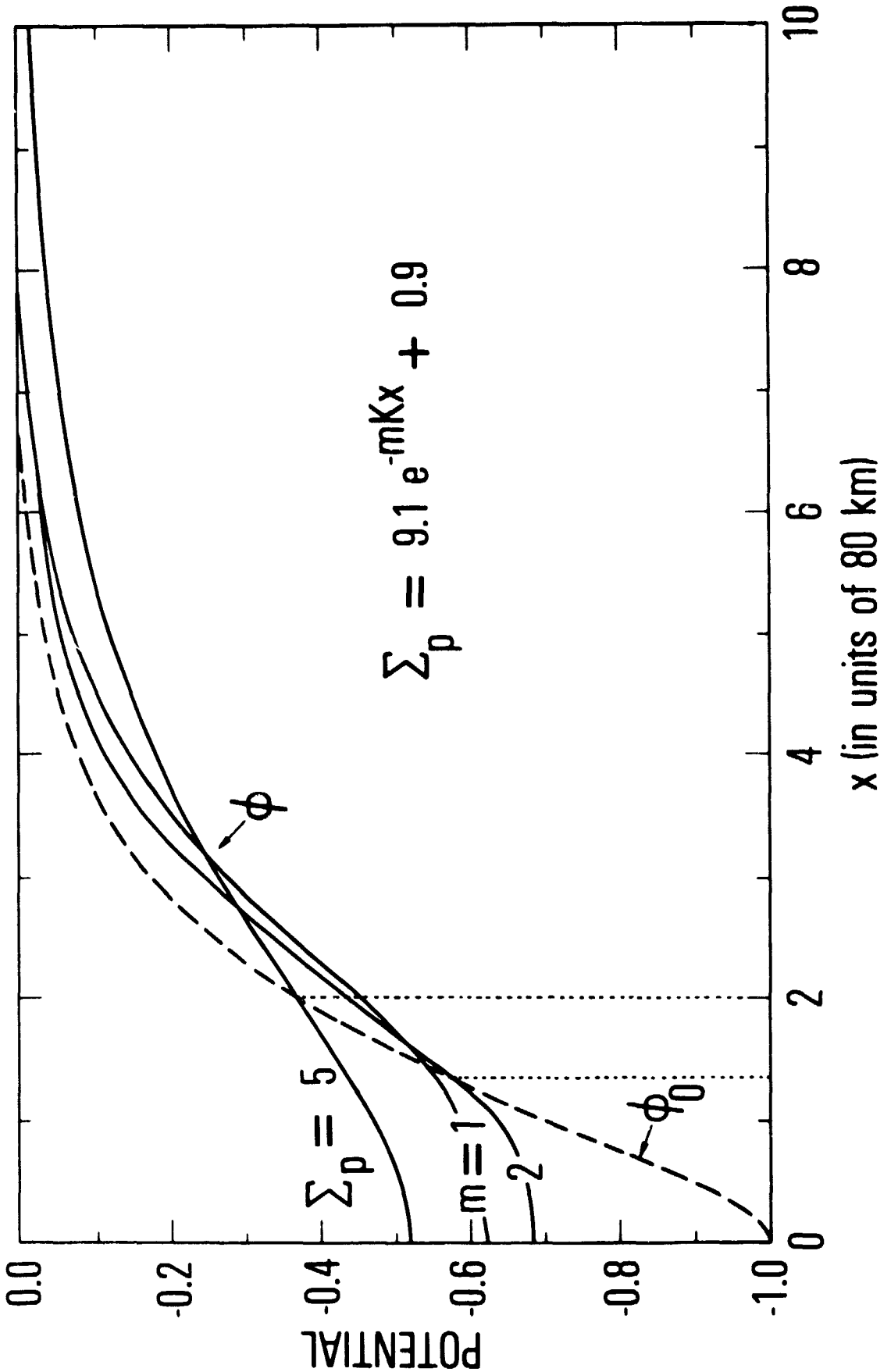
POTENTIAL
0.0
-0.2
-0.4
-0.6
-0.8
-1.0
0
2
4
6
8
10
x (in units of 80 km)
$\Sigma_p = 9.1\, e^{-mKx} + 0.9$
ϕ
ϕ_0
$\Sigma_p = 5$
m = 1
2

Fig. 4

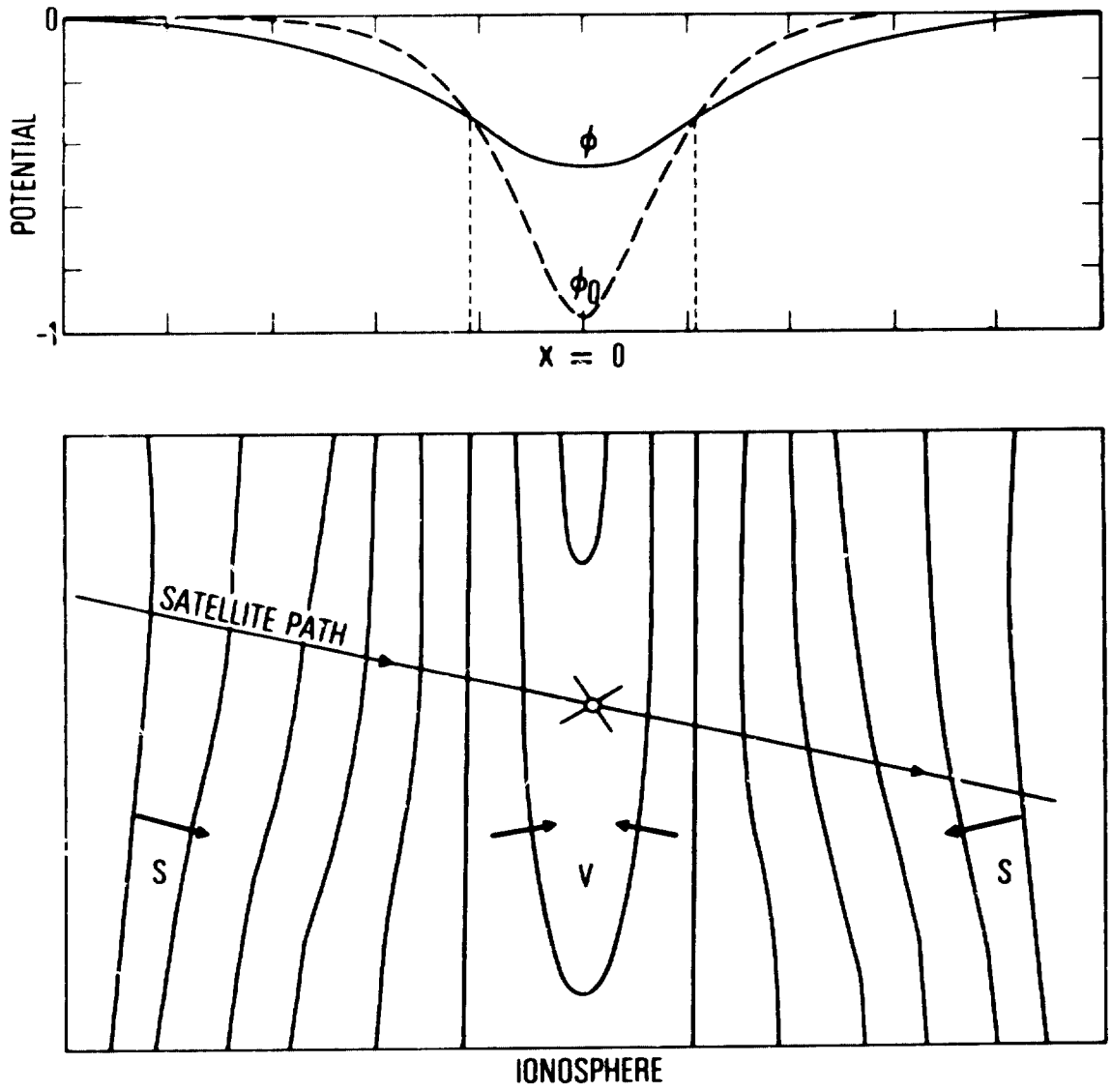

Fig. 5

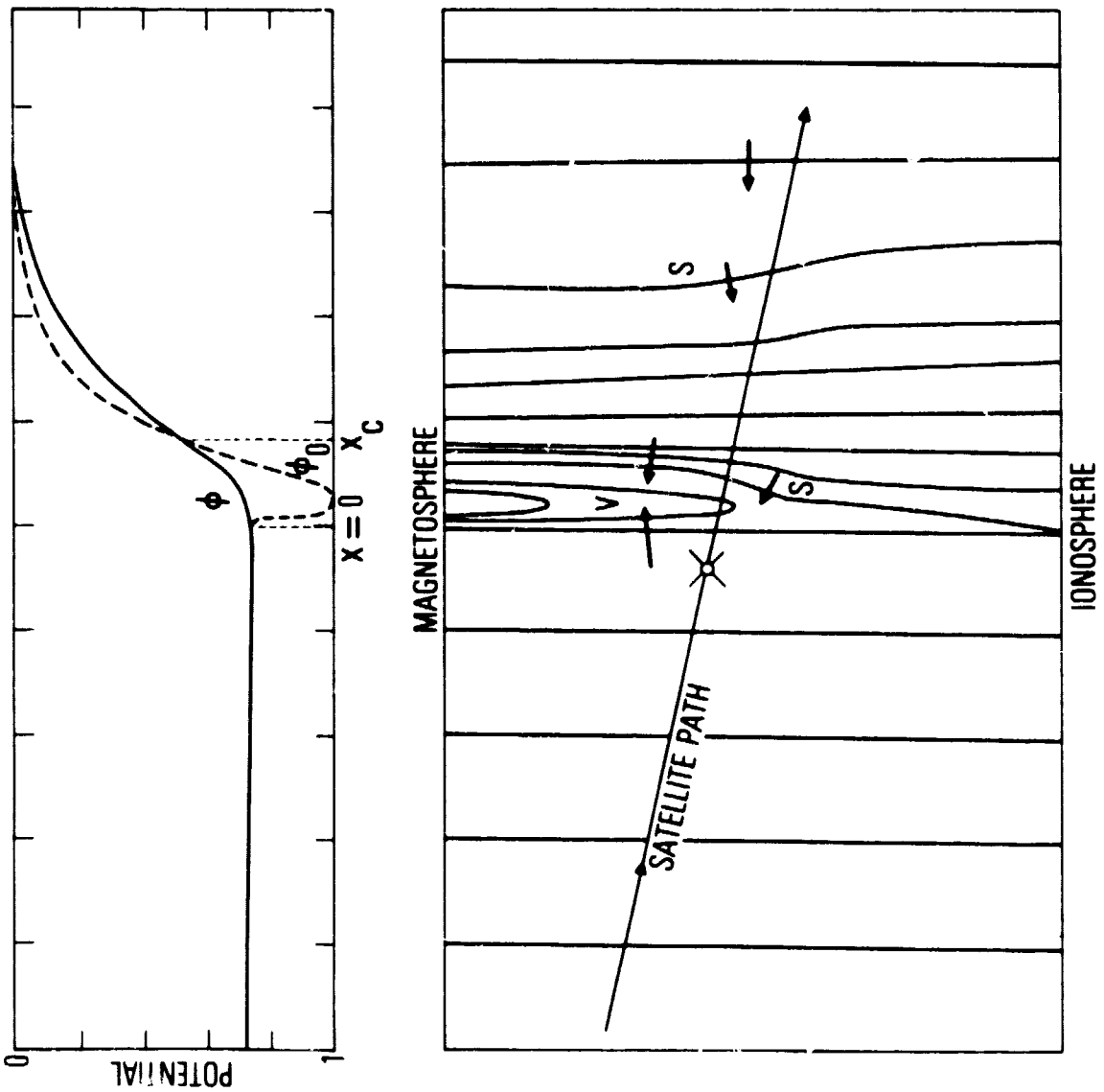
POTENTIAL
0
1
ϕ
ϕ_0
$x = 0$
x_c
MAGNETOSPHERE
IONOSPHERE
S
S
V
SATELLITE PATH

Fig. 6